Acta Mech 215, 211–224 (2010)
DOI 10.1007/s00707-010-0343-4

S. Casciati · R. Al-Saleh

Dynamic behavior of a masonry civic belfry under operational conditions

Received: 8 January 2010 / Revised: 11 April 2010 / Published online: 4 June 2010

Abstract Slender structures, such as towers, are characterized by a high sensitivity to dynamic excitation. As a consequence, meaningful information about their behavior under operational conditions can be obtained by monitoring their response to ambient vibrations. Furthermore, significant stresses could be induced to the ancient masonry walls when the dynamic forces due to the swinging of a bell are acting. To assess the structural conditions of a case study representative of such type of structures and to plan an adequate retrofit, numerical analyses are carried out on a model whose modal parameters are calibrated based on the elaboration of the results from the ambient vibrations tests. In particular, full time histories analyses are performed using as input either the signal recorded while the bell was hit by a hammer, or the numerically calculated dynamic forces that would be produced by the actual swinging of the bell. The first set of analyses aims to investigate the capability of an equivalent linear elastic model to capture the actual dynamic response of the structure. The second set of analyses provides an evaluation of the tower response when dynamic loads of higher intensity and likely occurrence are considered.

1 Introduction

High-rise buildings must be specifically designed to withstand the vibrations induced by wind loading. In new constructions, this task can be achieved by either adding dissipative devices [1] or by adopting an adaptive geometry [2]. Conceiving a monitoring system during the design phase of the building provides the advantage of assessing its actual performance with respect to the expected one accounting also for the deviations resulting from construction [3].

When historical masonry towers and belfries are considered, the difficulties related to an unknown structural state and to the requirement of non-invasiveness must be overcome. In Italy, the sudden collapse of the Pavia civic tower, in 1989, motivated the development of many research studies concerning these types of structures [4–15]. The results of these studies are peculiar to each structure under investigation, but they are the outcomes of a common three-step process that consists of the following: (a) monitoring, (b) diagnostics, and (c) retrofitting.

S. Casciati (✉)
Department of ASTRA, University of Catania, via Maestranza 99,
96100 Siracusa, Italy
E-mail: saracasciati@msn.com

R. Al-Saleh
Department of Structural Mechanics, University of Pavia, via Ferrata 1,
27100 Pavia, Italy

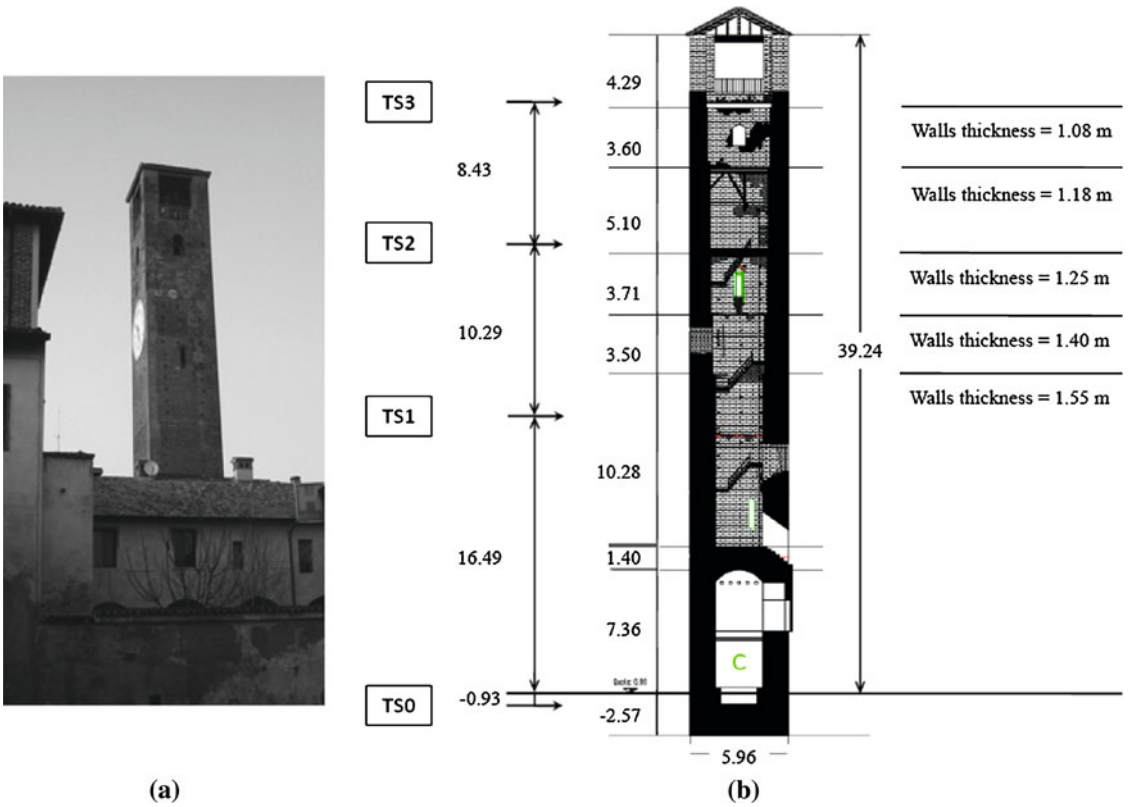

Fig. 1 The civic tower of Soncino: **a** picture of the southern side and **b** its geometric survey

The Soncino civic tower (Fig. 1a) provides an example of a case study to which such a three-step process was applied. As reported in previous studies [16–18,20–25], the tower was the object of a monitoring campaign whose results were elaborated toward diagnostics. The main outcome of these studies is the localization of an area where the tower is affected by passing cracks that influence its torsional behavior [17]. A non-invasive and reversible retrofit solution was proposed [20], and it is based on installing devices made of shape memory alloy wires at different levels of the damaged area. This retrofitting technique enables to strengthen the tower by confining its masonry blocks without preventing them from dissipating energy during vibrations [21]. The number of devices and their locations was established to optimize the retrofit in terms of both cost and performance. For this purpose, the comparison of the seismic vulnerability curves associated to each retrofitting solution was adopted as a criterion to assess the corresponding effects on the structural behavior [20]. This approach was pursued with a limited computational effort by adopting, for each considered structural configuration, a linear elastic model and a simplified procedure for the vulnerability assessment based on a single time history analysis [22]. For such a comparative purpose, a linear elastic finite element model could be sufficient, provided that the values of the equivalent Young's modulus are assigned so that the retrieved results are in agreement with the experimental data. The calibration of the initial (not retrofitted) model was pursued with reference to the modal parameters (natural frequencies and mode shapes) identified from the ambient vibration measurements during the diagnostics phase [17]. The results of laboratory tests on masonry specimens [18] were then used to numerically model the presence of the retrofitting devices by means of increases in the equivalent Young's modulus values in the interesting areas.

The described procedure is strongly dependent on the adequacy of the initial model in capturing the "dynamic signature" of the structure, which is independent of the entity and the type of the applied loads, but only depends on the intrinsic features of the structure, such as stiffness, damping, mass, and boundary conditions. The knowledge of the "dynamic signature" of a structure enables a better understanding of its structural scheme and an efficient design and planning of the maintenance and retrofit operations. For an existing structure, dynamic identification belongs to the class of the inverse problems, where the intrinsic features of the structure are unknown and must be determined from the experimentally measured structural response to specific loading conditions, which can either be assigned or are due to ambient vibrations. To solve the inverse

problem, an "ideal" model of the structure was implemented, and its mathematical formulation was targeted to retrieve at best the measured experimental data by adopting a "black box" approach, i.e., without considering any a priori knowledge. The resulting model is valid only if it is useful to interpret the monitored data and to enable a comparison with the experimentally measured dynamic response that is specific to the structure under consideration. In view of such a comparison, some model parameters were properly selected so that their iterative modifications enabled to perform a model updating at the end of which the target was reached with an acceptable error. Whether the solution of the identification problem is either unique, not unique, or not possible depends on the identifiability of the system, which must be taken under consideration within a case-specific context [19].

To further validate the results obtained for the case study of the Soncino civic bell tower, the present work focuses on investigating the capability of the resulting equivalent linear elastic model in capturing the "dynamic signature" of the structure as identified from the experimental data collected during its monitoring campaign. For this purpose, different segments of the recorded signals than those used for the modal parameters calibration are considered. In particular, the ones referring to the period of time in which a hammer was striking the bell at the top of the tower are used as inputs to perform full time histories analyses. The model validation consists of retrieving at the nodes located in correspondence with the lower sensor stations, response time histories that are in agreement with the experimental data. Once the model has been validated, it is used to evaluate the dynamic response of the structure under loading conditions of higher intensities. In particular, the most critical situation under normal operating conditions is identified with the one where the bell-swinging mechanism is activated. By repeating the analyses on a model whose material homogeneity has been restored, the results can be used to approximately quantify the benefits of a retrofit. Before implementing the retrofit, it is desirable to numerically assess the structural effects of different retrofitting solutions, thus enabling an optimal retrofit design [16].

2 Case study description and results from previous studies

Soncino is a small medieval village of about 9,000 inhabitants. It was established during the Germanic invasions that caused the end of the Roman Empire. During the Middle Ages, it played an important role as a fortress, due to its strategic position in the center of Northern Italy, along the eastern side of the river Oglio dividing the areas under the influences of Milan and Venice. Nowadays, it is a tourist site of interest, but it also runs the everyday life of a village. The Civic Tower (Fig. 1a), which represents the main object of the present study, was erected in 1128 within the fortification walls surrounding the medieval village. As often in these villages, the tower is located at the center of the urban nucleus, and it is surrounded by important buildings, such as the town hall and the public library. Furthermore, it was embedded for 10 m of height into the so-called Pretorius Palace, and nowadays it represents the only original part preserved.

2.1 Geometric survey

The tower (Fig. 1b) has a hollow square cross-section of exterior side equal to 5.96 m. The thickness of the masonry walls varies with the height, decreasing from 1.55 m at the bottom to 1.08 m at the top. At an elevation of 7.36 m from the ground level, there is a masonry vault ceiling of thickness 1.4 m. Adjacent buildings of 10 m height are located on three of the tower exterior sides, while the northern one gives on a road accessible to the vehicles traffic.

The structure originally constructed in 1128 A.D. had an initial height of 31.5 m. In 1575, its height was elevated up to 39.24 m by adding the bell room at the top. At present, the bell room consists of a concrete slab of thickness 0.15 m located at the height of 34.95 m and surmounted by four corner pillars supporting a roof. Two clocks are also mounted on the eastern and western sides of the tower.

2.2 Monitoring campaign

In 2000, the distributed cracks affecting all four sides of the tower exterior facade caused concerns about its potential collapse and justified an experimental campaign based on both visual inspections and the deployment of monitoring systems [23,24]. The internal accessibility of the tower enabled the installation of sensors at

different levels along its height (Fig. 1b). In particular, four stations each equipped with an uni-axial accelerometer, Kinemetrics FBA-11, working in parallel with a tri-axial velocimeter, Lennarz, Le-3D/5s were deployed as follows: TS0 at −0.93 m, TS1 at 16.5 m, TS2 at 26.8 m, and TS3 at 35.2 m from the ground level. Environmental vibrations were used as excitation method. Segments of the acceleration records were processed in order to identify the first five natural frequencies of the tower [25]. Their values are reported in the second column of Table 1. The corresponding mode shapes in the first column of Table 1 are referred to a Cartesian orthogonal coordinate system (O, x, y, z), whose y-axis is chosen along the shortest side of the building, the x-axis denotes the other horizontal direction, and the z-axis is in the vertical direction. A sketch of the adopted reference system is given in Fig. 2b.

2.3 Finite elements models

A homogeneous linear elastic finite element model [25] of the tower and parts of its surrounding buildings (Fig. 2a) is initially developed using SAP2000® version 10 [26] by uniformly setting the equivalent Young's modulus of the tower masonry equal to 2400 MPa. The mass density of the masonry is 1800 kg/m^3, and its Poisson's ratio is 0.17. In all the analyses discussed in this paper, the presence of a bell at the top of the tower is considered by lumping its mass and its inertial properties into the central node at the top of a steel frame supporting the bell weight. The modal analysis of the initially homogeneous model provides the values of the first five natural frequencies reported in the last column of Table 1. From the comparison with the experimental ones, the highest discrepancies are observed between the frequencies associated with the torsional mode. A sensitivity analysis [17] reveals that a change in the Young's modulus values assigned to the elements forming the tower walls of constant thickness right above the roof level of the surrounding buildings leads to a closer agreement with the experimental data, but it is not sufficient to capture the observed torsional behavior. Within a linear elastic context, the desired torsional mode can only be achieved by changing the geometry of the identified critical area. After several trials [27], an agreement with the experimental data is obtained by adopting the finite element model shown in Fig. 2b, which is characterized by an equivalent Young's modulus of the tower masonry equal to 3400 MPa everywhere, except in the four pillars resulting from removing clusters of

Table 1 Experimental and numerically calculated first five natural frequencies

Mode	Frequency [Hz]		Mode	Frequency [Hz]
	Experimental	Modified model (Fig. 2b)		Homogeneous model (Fig. 2a)
I. Bending along y	1.05	1.0493	I. Bending along y	1.0787
II. Bending along x	1.15	1.1682	II. Bending along x	1.2961
III. Torsion	2.5	2.8546	III. Bending along y	4.2582
IV. Bending along y	4.1	4.2650	IV. Bending along x	4.6721
V. Bending along x	4.3	4.4864	V. Torsion	4.8873

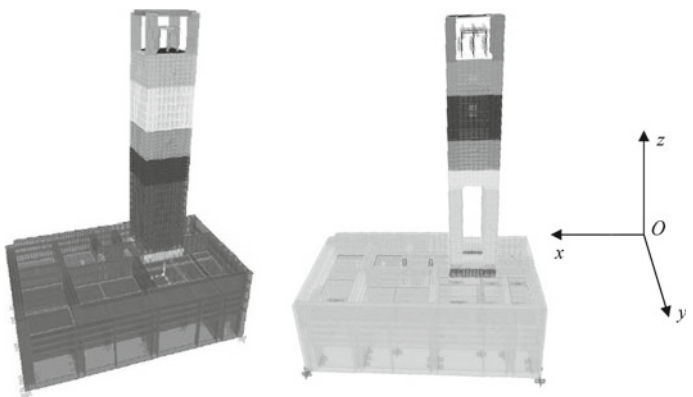

Fig. 2 Finite element models of the structures: **a** homogeneous and **b** modified model. Different shades characterize the walls forming rings of constant thickness

Table 2 Material properties assigned to the model of Fig. 2b

Elements typology	Material	Mass density [kg/m^3]	Young's modulus [MPa]	Poisson's ratio
Walls of the tower outside of the critical area	Masonry	1,800	3,400	0.17
Fictitious pillars within the critical area	Masonry	1,800	3,900	0.17
Walls of the surrounding buildings	Masonry	1,800	2,400	0.17
Floor slabs	Concrete	2,500	28,500	0.2
Frame supporting the bell at the top of the tower	Steel	7,850	210,000	0.3

elements from the critical area, where a higher value of 3900 MPa is assigned. The associated first five natural frequencies are listed in the third column of Table 1. A summary of the material properties characterizing the finite element model calibrated on the basis of the experimental frequencies (Fig. 2b) is provided in Table 2.

3 Model validation through dynamic analysis

The modified finite element model of Fig. 2b was obtained based on the experimental frequencies identified from the ambient vibrations data [28]. A further validation of such a numerical model is now pursued by considering datasets collected during different time periods of the same monitoring campaign. For this purpose, the displacement time histories measured in all three directions by the velocimeter Lennarz, Le-3D/5s, of station TS3, during the period of time in which a hammer was striking the bell at the top of the tower, are assigned as inputs to the dynamic analysis. The signals are referred to the same coordinates system of Fig. 2b, with the x-axis along the longest side of the building in which the tower is embedded. The hammer strikes are oriented in the x-direction; the time histories of the corresponding cinematic quantities are shown in Fig. 3. The excitation at the bell level was not recorded, so that the plots in Fig. 3 represent the tower response at the base of the steel frame supporting the bell as monitored by the sensors of station TS3. It is worth noting that the recorded signals result from the interaction between the bell response to the hammers strikes, the motion of the steel

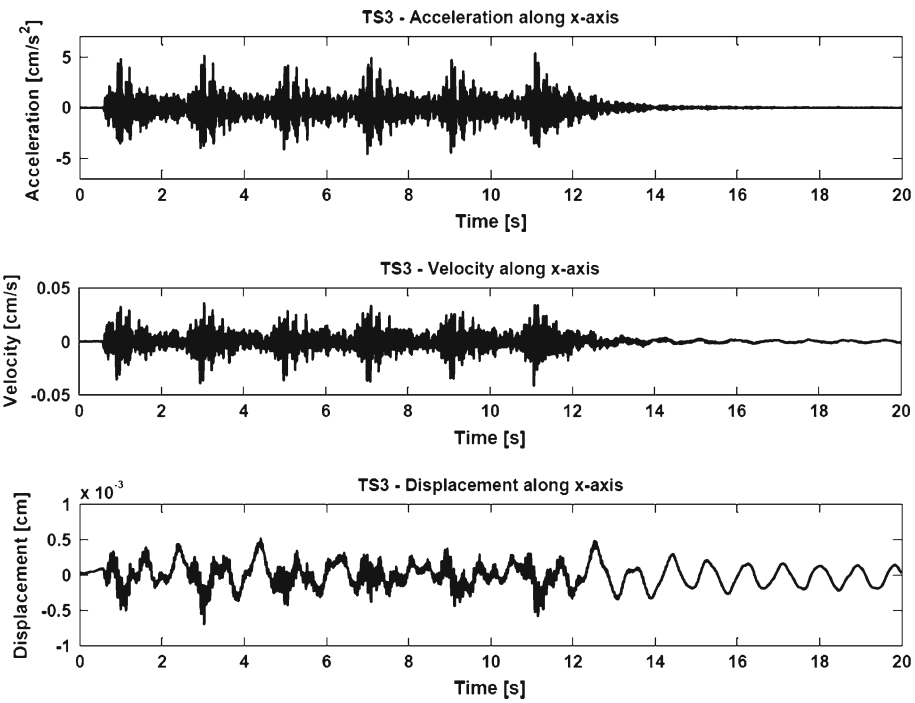

Fig. 3 Input data used for the dynamic analysis

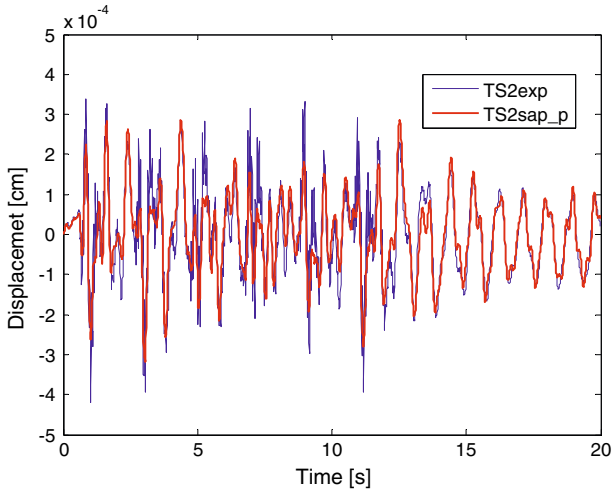

Fig. 4 Comparison of the displacement time histories along the *x*-axis: the displacements derived from the experimental data collected at station TS2 are plotted together with the ones numerically calculated at the corresponding node of the model in Fig. 2b

frame supporting the bell, and the motion of the main structure. The effects of the coupled dynamical systems are, therefore, implicitly included in the full time histories analysis by assigning these signals as inputs.

The acceleration time history of Fig. 3 is obtained by filtering the signal recorded at 6 a.m. along the *x*-axis by the velocimeter Lennarz, Le-3D/5s, placed at station TS3. The six spikes caused by the hammer striking the bell with a period of every 2 s are clearly detectable. The filtering was performed using the MATLAB® System Identification Toolbox [29]. Only the frequency content between 0.45 and 30 Hz was preserved by applying a pass band filter to the recorded signal. After double integration, one obtains the displacement time history that is also shown in Fig. 3. The filtering procedure is identically applied to process the signals recorded in the *z* and *y* directions. The corresponding displacement time histories are included in the analyses for the sake of completeness, but they are only representative of the background noise.

The displacement time histories derived from the records of station TS3 in all three directions are assigned as inputs to the dynamic analysis. Within the finite elements code SAP 2000, this procedure requires the introduction of a roller, in correspondence to which the given time history can be specified as a varying time boundary condition in each of the three directions. In order to avoid any fictitious torsional behavior of the tower, in the finite element model of Fig. 2b the same time histories are given at four rollers located at the midpoints of the opposite sides of the concrete slab at the top of the tower.

The dynamic analysis provides the structural response in the form of the displacement time histories numerically calculated at different nodes along the tower height. These results can be compared to the experimental data recorded, during the same period of time, by the remaining sensors placed along the tower height, after applying to them a preliminary signal-processing procedure analogous to the one performed on the records from station TS3. The displacement time history along the *x* direction derived from the signal recorded at station TS2 is plotted in Fig. 4. It shows a very good agreement with the one numerically obtained at the corresponding node from the dynamic analysis. Therefore, it can be concluded that the numerical model of Fig. 2b is able to accurately simulate the dynamic behavior of the structure outside its damaged area. For the sake of completeness, the tails of the experimental displacements derived from the records collected at station TS2 along the *y*- and *z* axes are drawn in Fig. 5, together with the corresponding ones calculated from the dynamic analysis. Despite the very low values of these displacements, it is possible to observe in the plots oscillations that are characterized by two main frequencies, which are associated to the tower and to the hammer, respectively.

Similar comparisons of displacement time histories cannot be pursued at station TS1, which is located within the damaged region. Indeed, the corresponding node is not present in the model of Fig. 2b, due to the elements removal from the critical area. Nevertheless, the displacement time histories numerically calculated at the same level of station TS1 in correspondence with the inner nodes of the four fictitious corner pillars of Fig. 2b show a satisfactory trend which is in agreement with the experimentally observed one.

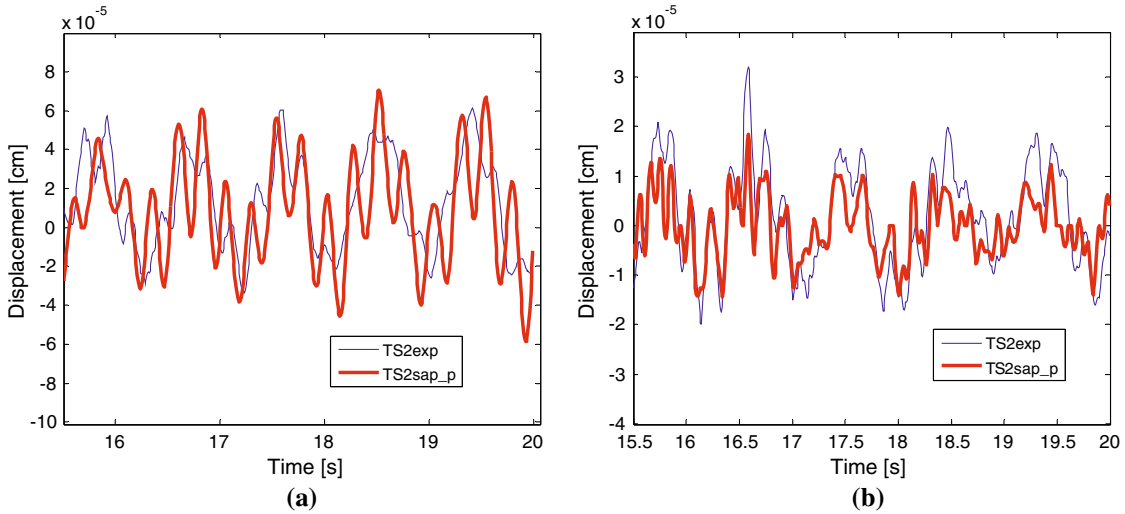

Fig. 5 Comparison of the displacement time histories derived from the experimental data collected at station TS2 with the ones numerically calculated at the corresponding node of the model in Fig. 2b: **a** displacements along the *y*-axis; **b** displacements along the *z*-axis

4 Bell forces calculation

The actual motion of the bell due to its swinging about its support point was not measured during the monitoring campaign, but it is in this circumstance that the maximum stresses due to normal operational conditions develop within the tower. Therefore, the functional objective of the retrofit design consists of a reduction in these stress values. To quantify such a benefit, a numerical simulation of the effects of the bell-swinging motion on the tower is performed by calculating the equivalent dynamic forces acting on the steel frame node where the bell mass is lumped. The present Section is dedicated to outline the procedure and the assumptions based on which the analytical expressions of the equivalent dynamic forces are derived. In literature, several different procedures are reported as suitable to approach the same problem with levels of accuracy whose adequacy depends on the considered case study. In particular, the inertial properties of the bell and its swinging system play an important role in adopting the proper assumptions.

The swinging mechanism of the bell in Fig. 7 is named "a sbalzo" or "alla Romana", and it does not include any counter weight. The bell never reaches an upside down position (called the "drinking glass" position), but it moves through an arch of about 90° in both directions, with a center of rotation approximately located at the height of its support. Hence, the supporting structure is expected to undergo significant thrusts during the bell oscillations. An approximate prediction of the forces transferred to the tower by the bell-swinging motion can be achieved by considering the undamped free motion of a physical pendulum under large oscillations. The dissipating effects of friction and the partly forced bell motion, together with the nonlinear effects induced by the coupling of the bell behavior with the motion of the main structure [30], prevent a precise estimate of these forces. For the Soncino case study, the swinging motion of the bell could not be measured, because it only occurs on special occasions. Nevertheless, in Beconcini et al. [31] and Cointe et al. [32], the actual motion of the bell was measured from accelerometric records of similar case studies, and the discrepancies detected with respect to the one numerically simulated by adopting such an approximate, uncoupled approach were found to be small. In particular, the results in Cointe et al. [32] refer to a bell supported by a timber frame, and they show that the kinematics of the horizontal displacements and the amplitudes of the motion can be satisfactorily represented under the frictionless and uncoupling assumptions. The lack of an accurate estimate of the actual period of the bell-swinging motion suggests to adopt a similar approach also for the Soncino case study.

Although a bell and a clapper form a coupled system of two pendulums [33], for the presented case study the bell motion can be approximated as a single compound pendulum [32,34] due to the small mass of the clapper, $M_c = 48.82\,\text{kg}$, in comparison with the one of the bell, $M_b = 2441\text{kg}$. The mass of the compound pendulum is assumed equal to the total mass of the coupled system, $M = M_b + M_c = 2489.82\,\text{kg}$. By considering the rod of an extended size, instead of mass-less, a compound pendulum (also called a "physical pendulum" in literature) consists of an arbitrarily shaped rigid body swinging by a pivot. From the geometric

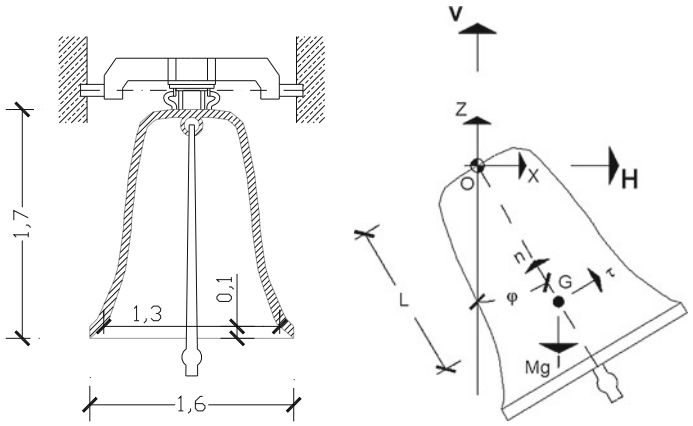

Fig. 6 **a** Geometry of the bell and **b** kinematics of the bell together with the dynamic forces acting on it

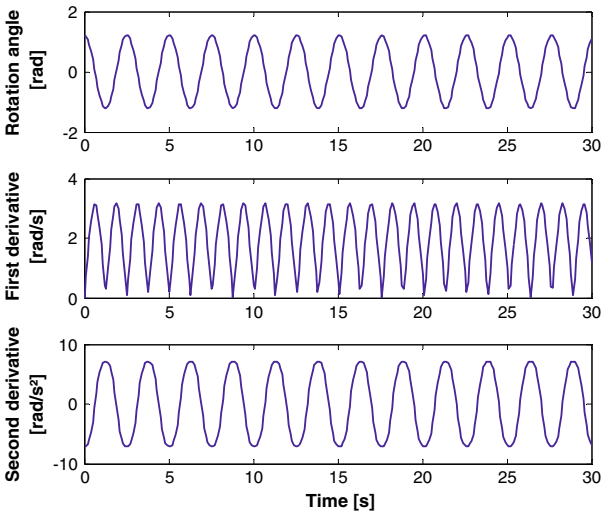

Fig. 7 Variation with time of the bell rotation angle (top) and of its first two derivatives

survey of the bell in Fig. 6, the distance, L, between the center of mass, G, and the pivot point, O, is equal to 0.9318 m. The moment of inertia of the bell about its rotation axis y is calculated as $I_y = 3100.82\,\mathrm{kg\,m^2}$.

Let $\varphi(t)$ the rotation angle formed by the bell axis of symmetry with respect to the vertical axis, z, as the bell position varies with time, t. The standard procedure of denoting with a dot each time derivative of a quantity is adopted. From the balance of moments about the pivot point, one derives the well-known equation of motion of a compound pendulum in free oscillation and large displacements,

$$\ddot{\varphi} + \omega^2 \sin\varphi = 0, \tag{1}$$

which is a nonlinear, second-order differential equation, with $\omega = \sqrt{MgL/I_y}$. The initial conditions are assumed as follows:

$$\varphi(t=0) = \varphi_0 = \varphi_{\max}; \quad \dot{\varphi}(t=0) = 0, \tag{2}$$

where the initial angle φ_0 is equal to 70° for the considered case study. Let $k = \sin(\varphi_0/2)$. The solution of Eq. (1), whose mathematical derivation can be found in Verhulst [35], is given by

$$\varphi(t) = 2\arcsin[k\,\mathrm{sn}(\omega t + C)], \tag{3}$$

where sn(.) denotes the Jacobi elliptic function, which represents the inverse of an incomplete elliptic integral of the first kind. The constant C is obtained by imposing the initial condition at $t = 0$, and it coincides with

the complete elliptic integral of the first kind, which also represents the quarter period of the Jacobi elliptic function, sn(.).

Figure 7 shows the variation with time of the bell rotation angle and of its first two derivatives. It is obtained using the MATLAB built-in functions "ellipke" and "ellipj" to compute the elliptic integral, $C = \text{ellipke}(m)$, and the elliptic function, $\text{sn}u = \text{ellipj}(u, m)$, respectively, with $u = \omega t + C$ and $m = k^2$.

The tangential and radial components of the acceleration vector of the center of mass of the bell can then be computed by multiplying the second time derivative and the square of the first time derivative of $\varphi(t)$ in Eq. (3) by the distance L of the center of mass from the pivot point, respectively. The corresponding acceleration components along the horizontal and vertical axes are achieved by simply applying the rotation formula. The equivalent dynamic forces are proportional to these components through the mass M of the compound pendulum. As a result, the following expressions are found for the horizontal and vertical forces acting on the pendulum at the pivot point O:

$$H = -ML\omega^2 \sin\varphi \left\{\cos\varphi + 4[k^2 - \sin^2(\varphi/2)]\right\}, \tag{4.1}$$

$$V = ML\omega^2 \left\{-\sin^2\varphi + 4[k^2 - \sin^2(\varphi/2)]\cos\varphi\right\} + Mg, \tag{4.2}$$

respectively. Plots of the corresponding time histories are shown in Figs. 8 and 9, respectively.

5 Estimate of the retrofit benefit in terms of the maxima Von Mises stresses in the tower under operational conditions

The identified numerical model of Fig. 2b, which was validated in Sect. 3, is now used to estimate the safety margin associated to the tower under operational conditions in its currently damaged situation. For this purpose, the dynamic forces in Figs. 8 and 9 are assigned as inputs to the node corresponding to the pivot point of the bell. Thus, full time histories analyses are performed to estimate the stress distributions induced in the damaged area under the combined actions of the tower self-weight and the dynamic forces due to bell-swinging motion. The integration time step is selected as $\Delta t = 0.008$ s, and the modal damping is assigned equal to 0.025.

From a graphical plot of the von Mises stress distribution in the tower, the corner elements indicated in Fig. 10 at the level of 10.81 m are detected as the most critical ones under the dead load condition. In Table 3, a summary of the stress values computed at the nodes of these corner elements is provided. For the sake of conciseness, only a single node of the element labeled 2038 in Fig. 10 is selected for the graphical representation of the results. Details of the geometry and nodes of this element are shown in Fig. 11, where its location within the mesh of the tower is also indicated. The belfry in its present damaged state shows a cumulating trend of the stress under the bell excitation, which leads to von Mises stress values larger than one half of those

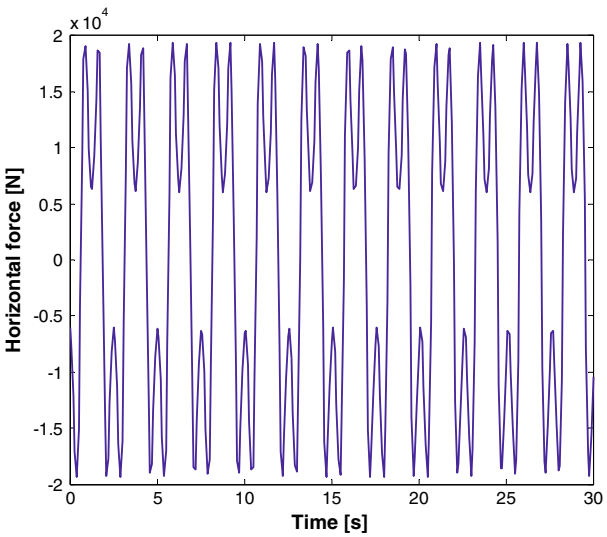

Fig. 8 Time history of the horizontal bell force for an initial angle of 70°

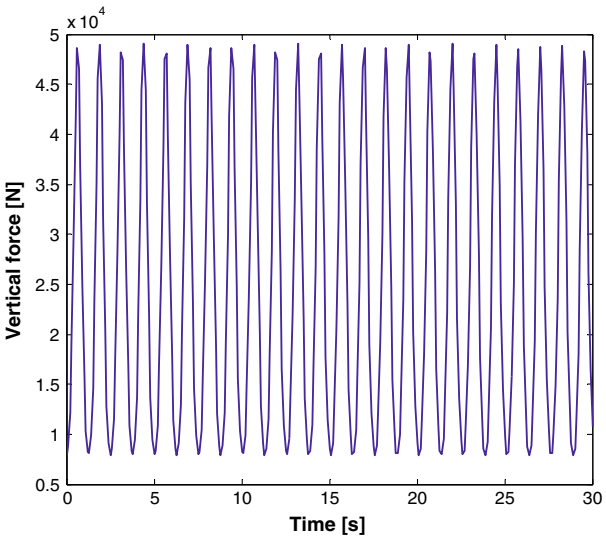

Fig. 9 Time history of the horizontal bell force for an initial angle of 70°

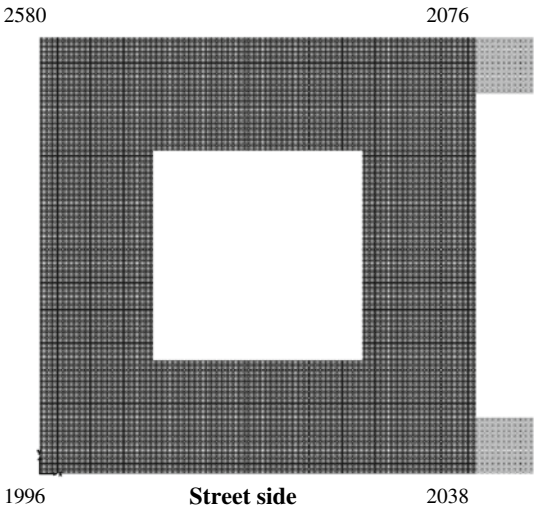

Fig. 10 Location of the eight nodes solid elements selected for the comparison of the Von Mises stress values in Table 3. The tower cross-section is drawn at the level of 10.81 m

detected under the dead load. To illustrate this statement, the Von Mises stress time history computed at node 1230 of element 2038 is drawn in Fig. 12.

If the retrofit whose details are discussed in references [21,22] is adopted, its presence can be modeled by replacing the zone identified as damaged in Fig. 2b with a homogeneous solid extension whose equivalent Young's modulus is set equal to the one characterizing the rest of the mesh elements modeling the tower (3,400 MPa). A consequent reduction in the Von Mises stress is detected as reported in the last three columns of Table 3. Following the retrofit, the main observed benefit consists of the fact that the oscillations of the bell do not produce a cumulating stress in the tower, so that the corresponding von Mises stress value reduces to one-tenth of the one associated with the current damaged state response. To illustrate this aspect, the time history response calculated after the retrofit, at the same node of Fig. 11, is drawn in Fig. 13.

6 Conclusions

A dynamic identification procedure was applied to the case study of the civic bell tower in Soncino, north of Italy [20]. In this paper, the validation of the resulting finite element model is pursued based on the signals

Table 3 Stress response of the tower under the dead load and the bell dynamic excitation, in its current damaged state and after retrofit. SVM denotes the von Mises stress, while $\sigma_{33}$is the normal stress along the vertical direction

Element	Node	Current belfry			After retrofit		
		Dead SVM [kN/m^2]	Bell max σ_{33} [kN/m^2]	Bell min σ_{33} [kN/m^2]	Dead SVM [kN/m^2]	Bell max σ_{33} [kN/m^2]	Bell min σ_{33} [kN/m^2]
1992	4895	604.81	299.41	−299.41	449.18	35.75	−39.03
	4896	629.18	95.67	−96.04	495.02	28.2	−31.78
	4900	537.27	296.41	−296.42	378	36.04	−39.35
	4901	593.30	92.13	−92.48	452.34	27.71	−31.22
	1220	619.05	285.94	−285.71	458.43	35.53	−38.84
	4897	670.28	91.09	−91.24	534.95	29.06	−32.92
	1221	537.73	289.49	−289.27	382.71	36.02	−39.4
	4902	618.27	94.09	−94.23	486.5	28.77	−32.59
2038	4946	506.57	77.09	−78.02	395.46	31.86	−33.42
	4948	773.29	424.63	−426.38	663.67	67.49	−69.47
	4951	685.98	89.7	−90.68	516.62	33.71	−35.31
	4953	907.57	439.31	−441.15	760.65	70.92	−72.97
	4947	490.13	72.46	−73.03	473.02	32.42	−34
	1230	820.48	469.47	−470.99	776.38	79.71	−82.02
	4952	615.44	57.8	−58.28	493.1	28.99	−30.5
	1231	953.89	456.86	−458.33	847.82	77.85	−80.12
2076	4990	683.08	388.65	−391.12	557.01	65.8	−66.82
	4991	474.07	65.98	−67.63	352.96	31.13	−32.26
	4995	788.65	401.69	−404.24	602.22	68.94	−70.03
	4996	649.77	78.66	−80.37	443.87	32.67	−33.83
	1248	775.53	446.74	−449.87	676.83	81.22	−82.52
	4992	476.98	66.43	−68.27	407	32.92	−34.08
	1249	879.45	434.07	−437.13	722.44	79.68	−80.95
	4997	614.51	53.39	−55.14	453.81	29.78	−30.87
2576	5585	698.46	108.15	−109.58	542.58	34.36	−38.12
	5586	658.49	105.92	−107.04	494.7	32.31	−35.81
	5590	641.23	110.81	−112.22	494.52	33.98	−37.7
	5591	612.95	102.59	−103.7	457.48	31.77	−35.2
	1238	651.79	301.32	−302.31	465.66	39.21	−42.39
	5587	647.54	310.64	−311.4	451.71	38.99	−42.2
	1239	562.49	304.64	−305.64	390.15	39.75	−43.01
	5592	568.67	307.98	−308.76	385.36	39.36	−42.61

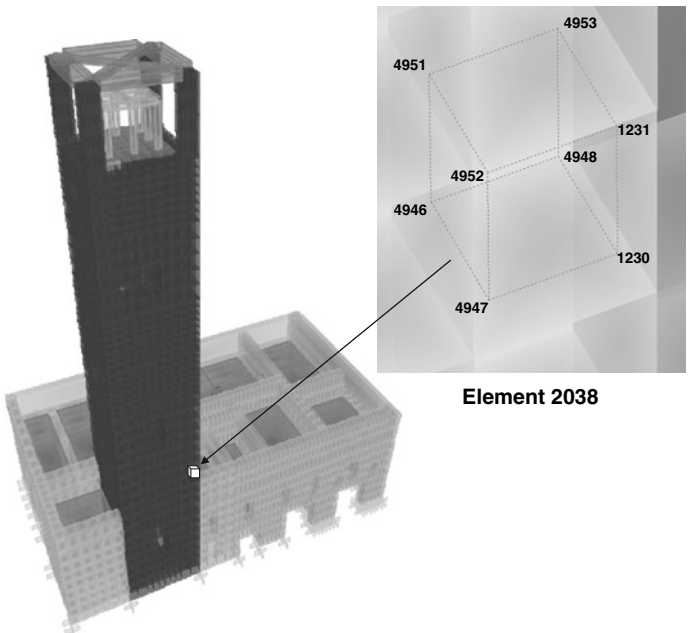

Fig. 11 Details of the geometry and nodes of element 2038, whose node labeled 1230 is selected for the graphical representations of the results in Figs. 12 and 13

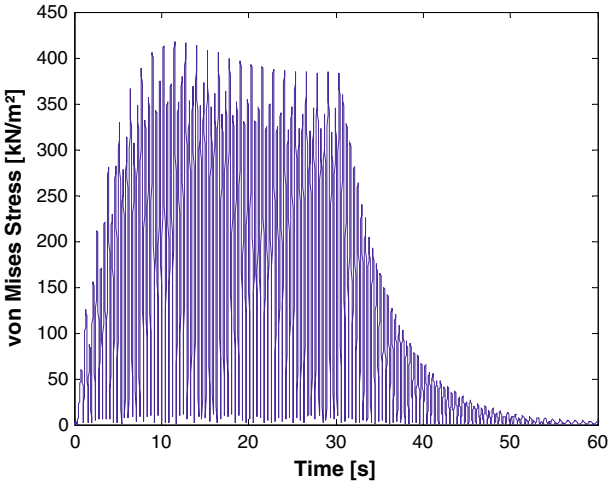

Fig. 12 Von Mises stress time history due the bell force excitation: current state (element 2038, node 1230)

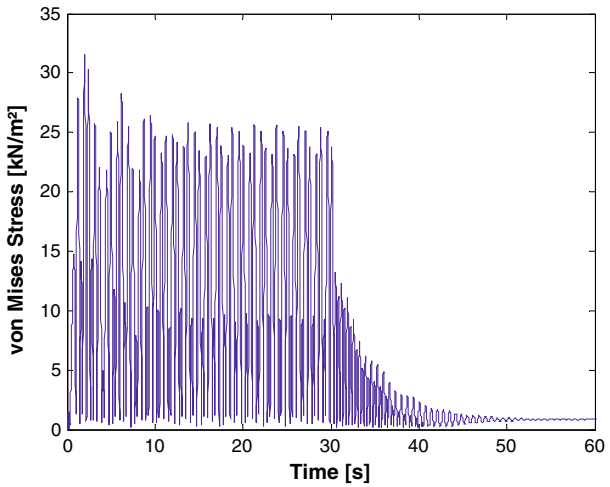

Fig. 13 Von Mises stress time history due the bell force excitation: retrofitted state (element 2038, node 1230)

recorded from a localized source of excitation, which consists of the repetitive impacts of a hammer on a bell located at the top of the tower. By assigning as inputs, the displacement time histories recorded at the closest station to the excitation source, the ones computed at the other nodes corresponding to sensors locations are compared to the experimentally measured ones.

The swinging motion of the bell is then considered in order to evaluate the maxima stresses in the tower under its operational loading conditions. Such a motion was not experimentally measured, because it occurs only on special occasions. Therefore, the produced dynamic forces have been numerically calculated based on the bell geometry and on its swinging system. The approximation of the behavior of the bell-clapper system as the one of a compound pendulum is legitimated by the small mass of the clapper with respect to the one of the bell. The calculated bell forces are assigned to the interested nodes of the finite element model to evaluate the time histories of the Von Mises stress at the most critical nodes of the validated finite element model. Finally, the potential benefits of a retrofit are investigated by repeating the analysis on a numerical model whose material homogeneity has been restored.

Acknowledgments This research is supported by the Athenaeum Research Funds from both the University of Catania (PRA 2008) and the University of Pavia (FAR 2009).

References

1. Cao, H., Reinhorn, A.M., Soong, T.T.: Design of an active mass damper for a Tall TV tower in Nanjing, China. Eng. Struct. **20**, 134–143 (1998)
2. Casciati, F., Faravelli, L., Al-Saleh, R.: Dynamic Architecture vs. Structural Control. In: Proceedings of Smart Structures and Materials (SMART'09) IV Eccomas Thematic Conference, Porto, Portugal, 13–15 July 2009
3. Ni, Y.Q., Xia, Y., Liao, W.Y., Ko, J.M.: Technology innovation in developing the structural health monitoring system for Guangzhou New TV tower. Struct. Control Health Monit. **16**, 73–98 (2009)
4. Anzani, A., Garavaglia, E., Binda, L.: Long-term damage of Historic Masonry: a probabilistic model. Constr. Build. Mater. **23**, 713–724 (2009)
5. Bennati, S., Nardini, L., Salvatore, W.: Dynamic behavior of a Medieval Masonry Bell Tower. II: measurement and modeling of the tower motion. J. Struct. Eng. **131**, 1656–1664 (2005)
6. Binda, L., Zanzi, L., Lualdi, M., Condoleo, P.: The use of georadar to assess damage to a Masonry bell tower in Cremona, Italy. NDT & E Int. **38**, 171–179 (2005)
7. Bonato, P., Ceravolo, R., De Stefano, A., Molinari, F.: Cross-time frequency techniques for the identification of Masonry buildings. Mech. Syst. Signal Process. **14**, 91–109 (2000)
8. Carpinteri, A., Lacidogna, G.: Damage evaluation of Three Masonry towers by acoustic emission. Eng. Struct. **29**, 1569–1579 (2007)
9. Gentile, C., Saisi, A.: Ambient vibration testing of Historic Masonry towers for structural identification and damage assessment. Constr. Build. Mater. **21**, 1311–1321 (2007)
10. Giannini, R., Pagnoni, T., Pinto, P.E., Vanzi, I.: Risk analysis of a Medieval tower before and after strengthening. Struct. Saf. **18**, 81–100 (1996)
11. Lucchesi, M., Pintucchi, B.: A numerical model for non-linear dynamic analysis of Slender Masonry structures. Eur. J. Mech. A/Solids **26**, 88–105 (2007)
12. Reale, E., Paguni, C., Floridia, S.: Static and dynamic analysis of S. Peter tower in Modica, Ragusa, Sicily, In: Lourenço, P. B., Roca, P. (eds.) Historical Constructions 2001: Possibilities of Numerical and Experimental Techniques, pp. 887–896. University of Minho, Guimarães, Portugal (2001). Available at: http://www.civil.uminho.pt/masonry/
13. Riva, P., Perotti, F., Guidoboni, E., Boschi, E.: Seismic analysis of the Asinelli tower and earthquakes in Bologna. Soil Dyn. Earthq. Eng. **17**, 525–550 (1998)
14. Sepe, V., Speranza, E., Viskovic, A.: A method for large-scale vulnerability assessment of Historic Towers. Struct. Control Health Monit. **15**, 389–415 (2008)
15. Valluzzi, M.R.: On the vulnerability of Historical Masonry structures: analysis and mitigation. Mater. Struct. **40**, 723–743 (2007)
16. Casciati, S., Hamdaoui, K. (2007) Optimal robust design via SMA dissipative devices, In: Applications of Statistics and Probability in Civil Engineering, Kanda, Takada, and Furuta, eds. Taylor & Francis Group, London, UK. ISBN: 978-0-415-45134-5
17. Casciati, S.: Monitoring data for the structural assessment of Historical buildings. In: Uhl, T., Ostachowicz, W., Holnicki-Szulc, J. (eds.) Structural Health Monitoring 2008 Proceedings Fourth European Workshop, pp. 227–233. Destech Publications Inc, Lancaster, Pa, USA (2008)
18. Casciati, S., Hamdaoui, K.: Experimental and numerical studies toward the implementation of shape memory alloy ties in Masonry structures. Smart Struct. & Syst. **4**, 153–169 (2008)
19. Casciati, S.: Stiffness identification and damage localization via differential evolution algorithms. Struct. Control Health Monit. **15**, 436–449 (2008)
20. Casciati, S., Faravelli, L.: Vulnerability assessment of Medieval civic towers as a tool for retrofitting design. In: Santini, A., Moraci, N. (eds.) Seismic Engineering International Conference Commemorating 1908 Messina and Reggio Calabria Earthquake, pp. 92–99. American Institute of Physics (AIP) Conference Proceedings, Melville, New York, USA (2008)
21. Casciati, S., Faravelli, L.: Structural components in shape memory alloy for localized energy dissipation. Comput. Struct. **86**, 330–339 (2008)
22. Casciati, S., Faravelli, L.: Vulnerability assessment for Medieval civic towers. Struct. Infrastruct. Eng. **6**, 193–203 (2010). doi:10.1080/15732470802664290
23. Marcellini, A., Tento, A., Daminelli, R., Poggi, V.: Tecniche sperimentali per la valutazione simultanea delle caratteristiche dinamiche di suoli e strutture. Internal Report (in Italian), Institute for the Dynamics of Environment Processes, National Research Council (CNR), Milan (2005)
24. Beccari, M.: Monitoraggio e Identificazione della Torre Civica di Soncino, Master Thesis (in Italian). Department of Structural Mechanics, University of Pavia, Italy (2006)
25. Persano S.: La Torre Civica di Soncino: modellazione e diagnostica. Master Thesis (in Italian), Department of Structural Mechanics, University of Pavia, Italy (2006)
26. SAP2000: Linear and Nonlinear Static and Dynamic Analysis and Design of Three-Dimensional Structures. Computers and Structures, Inc (1995)
27. Camerini, S.: Adeguamento strutturale della torre civica di Soncino e curve di fragilità. Master Thesis (in Italian), Department of Structural Mechanics, University of Pavia, Italy (2008)
28. Casciati, S., Al-Saleh, R.: Combining numerical methods with experimental data toward the structural rehabilitation assessment of ancient masonry landmarks. In: Mazzolani, F. (ed.) Protection of Historical Buildings, PROHITECH 09, pp. 1729–1734. Taylor & Francis, London (2009)
29. Ljung, L.: System Identification Toolbox 7 User's Guide. The MatWork, Inc. (2005)
30. Heuer, R., Yousefy, S.M.: Hybrid bell tower like structures in earthquake environment. In: Irschik, H., Krommer, M., Watanabe, K., Furukawa, T. (eds.) Mechanics and Model-based Control of Smart Materials and Structures, pp. 69–76. Springer, Wien (2010)

31. Beconcini, M. L., Bennati, S., Salvatore, W.: Structural characterization of a medieval bell tower: first historical, experimental and numerical investigations. In: Lourenço, P. B., Roca, P. (eds.) Historical Constructions 2001, Possibilities of Numerical and Experimental Techniques, Proc. 3rd Int. Seminar, Structural Analysis of Historical Constructions, Guimarães, Portugal, pp. 431–444 (2001)
32. Cointe, A., Castéra, P., Morlier, P., Galimard, P.: Diagnosis and monitoring of timber buildings of cultural heritage. Struct. Saf. **29**, 337–348 (2007)
33. Ivorra, S., Palomo, M.J., Verdú, G., Zasso, A.: Dynamic forces produced by bell swinging. Meccanica **41**, 47–62 (2006)
34. Lemmens, K., Rijnks, H.: Mathematical model for the bell SWI: project Old Church Delft (2004)
35. Verhulst, F.: Nonlinear Differential Equations and Dynamical Systems. 2nd edn. Springer, Berlin (1996)